Growth-mode and interface structure of epitaxial ultrathin MgO/Ag(001) films

Maurizio de Santis, V Langlais, K Schneider, X Torrelles

Growth-mode and interface structure of epitaxial ultrathin MgO/Ag(001) films

M. De Santis [1,*], V. Langlais[2], K. Schneider[2] and X. Torrelles[3]

[1] Université Grenoble Alpes, CNRS, Grenoble INP, Institut Néel, 38042 Grenoble, France
[2] CNRS, CEMES (Centre d'Elaboration des Matériaux et d'Etudes Structurales), B.P. 94347, 29 rue Jeanne Marvig, F-31055 Toulouse, France
[3] Institut de Ciència de Materials de Barcelona, ICMAB-CSIC, Bellaterra, 08193 Barcelona, Spain

*E-mail: maurizio.de-santis@neel.cnrs.fr

Received
Accepted for publication
Published

Abstract

MgO ultrathin films are of great technological importance as electron tunneling barrier in electronics and spintronics, and as template for metallic clusters in catalysis and for molecular networks for 2D electronics. The wide band-gap of MgO allows for a very effective decoupling from the substrate. The films morphology and the detailed structure of the interface are crucial for applications, controlling the electronic transfer. Using surface x-ray diffraction, we studied the growth-mode and the structure of MgO/Ag(001) ultrathin films elaborated by reactive molecular beam epitaxy as function of the substrate temperature. We observed that deposition of about 1 monolayer results in an MgO(001) film in coherent epitaxy, with the oxygen atoms on top of silver as predicted by DFT calculations, and an interlayer distance at the interface of about 270 pm. Under well-defined conditions, a sharp MgO bilayer is formed covering a fraction of the substrate surface.

Keywords: magnesium oxide films, epitaxial growth, ultrathin films structure, surface x-ray diffraction.

1. Introduction

Oxide surfaces and surface oxides play a fundamental role for a large number of important processes. All metals are generally covered by a thin native oxide film, and it is this oxide skin that governs their surface reactivity rather than the surface properties of the metal itself. In addition, oxides themselves are also used as catalysts and as supports for metallic cluster catalysts. The metal/oxide interfacial interactions that occur in the latter structures can have significative effects on catalyst performances.

The use of thin-films growth techniques to prepare model oxide surfaces is a field of fundamental science that has attracted more and more attention in the past decades [1]. The epitaxy of oxides on metals allows to synthetize crystalline films that in some cases can reach a high degree of perfection. The ability to engineer nearly perfect ultrathin oxide layers is a key issue for nanotechnological applications. From a fundamental point of view, their crystal structure allows to model and to reach a better understanding of the oxide and interfaces properties. In ultrathin films, the conductivity achieved through tunneling permits the use of electron-based techniques to investigate the structural and electronic properties of the films, interfaces and adatoms. Ultrathin insulating films provide also a precise electrostatic coupling and electron tunneling from a conducting substrate to a second electrode or to adsorbed nanostructures [2], which can be tuned choosing accurately the number of dielectric spacer layers [3].

Here we will discuss the growth of a well-defined and structurally ordered magnesium oxide (MgO) layer on top of the silver (001) surface. MgO is the insulating material of

choice in spintronic and is important in catalysis as template for metallic clusters. Growth of non-polar (001) oriented MgO films results in general in a high crystalline quality and in high performances e.g. as tunneling barrier [4]. MgO thin films on Ag(001) surface is a prototypical model system for the understanding of the metal-oxide interface due to the small lattice mismatch between the oxide and the metal, which results in a coherent growth for ultrathin films [5, 6]. Defect-free MgO (001) single crystal surface is practically inert, but low coordinated atoms at edge, step, corner, and kink sites can act as electrons donors. Moreover, reactivity can originate from the presence of trapped electrons in surface defect sites [7]. Electron transfer can be observed when molecules, metal atoms or clusters are deposited on the surface of an ultrathin film, even in the absence of defects. This is the result of electron tunneling through the thin oxide layer rending possible STM experiments [3]. It was shown both experimentally [8] and by DFT calculations [9] that Au atoms deposited on MgO(001) "thick" films are essentially neutral and keep their atomic character. On the contrary Au atoms adsorbed on a MgO ultrathin film are negatively charged [10, 11]. Ultrathin MgO films themselves exhibit improved properties as catalyst for chemical reactions compared to bulk MgO, e. g. for water dissociation [12]. Charge transfer through the MgO layer not only promotes the catalytic activity, but also control the properties of hybrid inorganic/organic interfaces of interest for optoelectronic [13].

Moreover, ultrathin insulating layers inserted between a metallic substrate and deposited atoms or molecules are employed to improve their magnetic properties. Magnetic remanence was recently observed up to a temperature of 30 kelvin in individual holmium atoms adsorbed on ultrathin MgO(001) layers on Ag(001) [14]. This extraordinary stability was achieved thanks to the decoupling of the Ho spin from the underlying metal by the MgO tunnel barrier, and is function of its thickness. In a similar manner, giant hysteresis was observed for single-molecule magnets adsorbed on MgO/Ag(001) [15]

Tailoring magnetic and catalytic properties and comparing experiments with theory require a precise control of the film growth and morphology down to the monolayer (ML) thickness and the realization of almost defect free layers. The electronic structure and morphology of ultrathin MgO films grown on Ag(001) under different conditions were studied by several groups using mainly XPS, STM or other scanning probe microscopy techniques [3, 16, 17, 18, 19, 20]. Island formation was observed in a large temperature interval, spanning from 373 K to 673 K [21]. A decreasing of the island density and an increasing of their size was found up to 573 K. At this temperature, the flattest and largest MgO islands were reported. This represents a compromise between a sufficiently high mobility of Mg and MgO molecules and a not too high one of Ag adatoms. Further increasing the temperature at 673 K, MgO dendrites formation was observed. Pal *et al*. have shown that MgO films morphology depends not only on the growth parameters values (crystal temperature, metal flux, and oxygen partial pressure), but also on aftergrowth treatments [19]. They observed a bilayer growth for films elaborated at 773 K followed by usual cooling conditions, which switches to monolayer growth if the film is submitted to a slow cooling.

Here we use surface x-ray diffraction (SXRD) to study the structure and morphology of about 1 ML thick MgO films grown on Ag(001) in the 620-720 K temperature range. SXRD is a unique tool to investigate in particular the interface structure. This last one impacts various electronic properties, like e.g. the work function of the system, which is

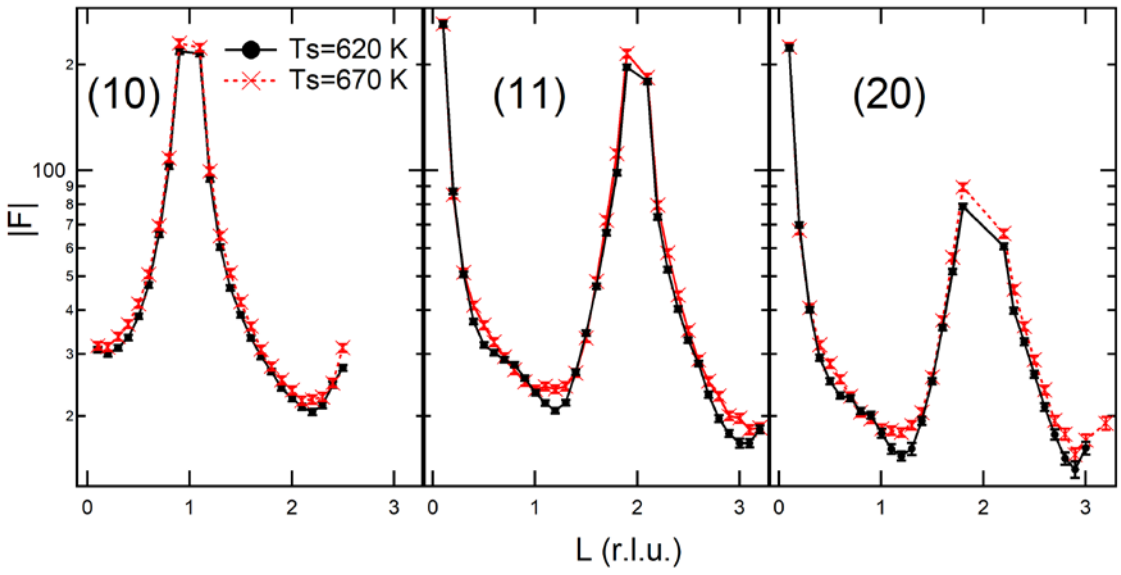

Figure 1. Experimental MgO/Ag(001) CTRs with error bar, measured after depostion of about 0.8 ML of Mg on Ag(001) in 10^{-6} mbar O_2 at T_s=620 K (filled black circles) and at 670 K (crosses, red online). The continuous lines are plotted for eyes guide.

particularly sensitive to the interfacial distance, or the position of the Fermi level within the oxide band gap [22 and references cited therein].

2. Experimental methods

The present experiment was performed at the European Synchrotron Radiation Facility (ESRF, Grenoble, France) using the dedicated In Situ Nanostructures and Surfaces (INS2) apparatus of the BM32 beamline. The x-ray source is a bending magnet and the monochromator is a Si(111) double crystal, with the second crystal bent to give sagittal focusing on the sample. The vertical focusing is provided by two mirrors, resulting in a spot size of about 0.2×0.3 mm^2. The experimental station consists of an ultrahigh vacuum chamber with base pressure in the low 10^{-10} mbar range and fully equipped for sample preparation, which is mounted on a Z-axis diffractometer. Further degrees of freedom are available to align the sample at the centre of the diffractometer and with the surface normal parallel to the sample azimuthal rotation axis. The measurements were performed at a photon energy of 19.8 keV, and at a grazing angle of 0.48° (except of course for the reflectivity). It corresponds to about three times the Ag critical angle for total reflection at this energy.

The polished surface of an Ag(001) single crystal (MaTeck, Jülich, Germany), with a 10 mm diameter and a miscut of less than 0.1°, was cleaned through successive cycles of Ar^+ ion sputtering and annealing at 800 K. The substrate temperature was measured using an infrared pyrometer. Cleanliness was checked by Auger electron spectroscopy (AES), such that all contaminants were below the detection limit. MgO was grown by reactive molecular beam epitaxy. Metallic Mg was evaporated by a water-cooled Knudsen cell, with the chamber backfilled with molecular oxygen at a partial pressure of 10^{-6} mbar. The magnesium flux had been previously calibrated by using a quartz crystal microbalance. The deposition rate was about 1 ML every 5 min, where we define 1 ML as the number of atoms in an Ag(001) plane. In these conditions the oxygen pressure largely exceeds the one needed for stoichiometric growth (see e.g. ref. [23]). Several samples were grown by evaporating the same amount of Mg, corresponding to a nominal thickness of 0.8 ML, at a substrate temperature T_s of 620 K, 670 K and 720 K, respectively. After deposition, the samples were cooled down below 450 K in less than 5 min, and O_2 pressure was removed while starting to cool down. The coverage and composition were checked by AES measuring the Ag *MNN*, O *KLL*, and Mg *KLL* Auger peaks at 356 eV, 513 eV and 1200 eV, respectively. Within the error bar, the intensity ratio of Mg and O peaks was the same for all samples, showing that the films have roughly the same stoichiometry. The Auger peaks of films grown at 620 K and 670 K had also roughly the same amplitude with respect to the substrate ones. Instead, the Mg and O peaks of the sample elaborated at 720 K were much weaker, showing that in this case most of Mg deposited is desorbed from the surface before a stable MgO layer can form. In previous studies [3, 21, 15], large flat islands with a low defects' density were observed on samples grown in close Mg flux and O_2 pressure conditions and at a temperature of about 500 K, 573 K, and 625 K, respectively. Other groups used higher deposition temperatures applying a higher local oxygen pressure thanks to a doser [19,37].

SXRD measurements were performed at room temperature to solve the structure of the samples elaborated at 620 K and 670 K. The data were collected using a 2D detector (MAXIPIX, ESRF).

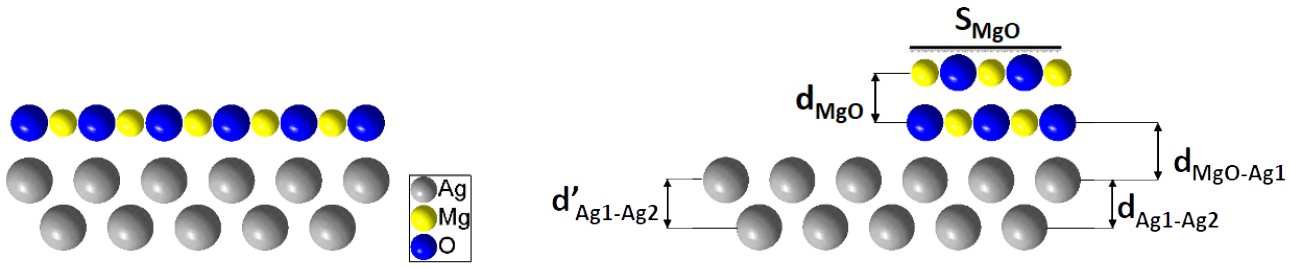

Figure 2. Sketches of the monolayer (left) and bilayer (right) models for MgO/Ag(001). On the right, the fitting distance and coverage parameters are indicated. $d_{Ag1\text{-}Ag2}$ and $d'_{Ag1\text{-}Ag2}$ represent the first Ag-Ag interlayer distance in MgO covered and uncovered regions, respectively.

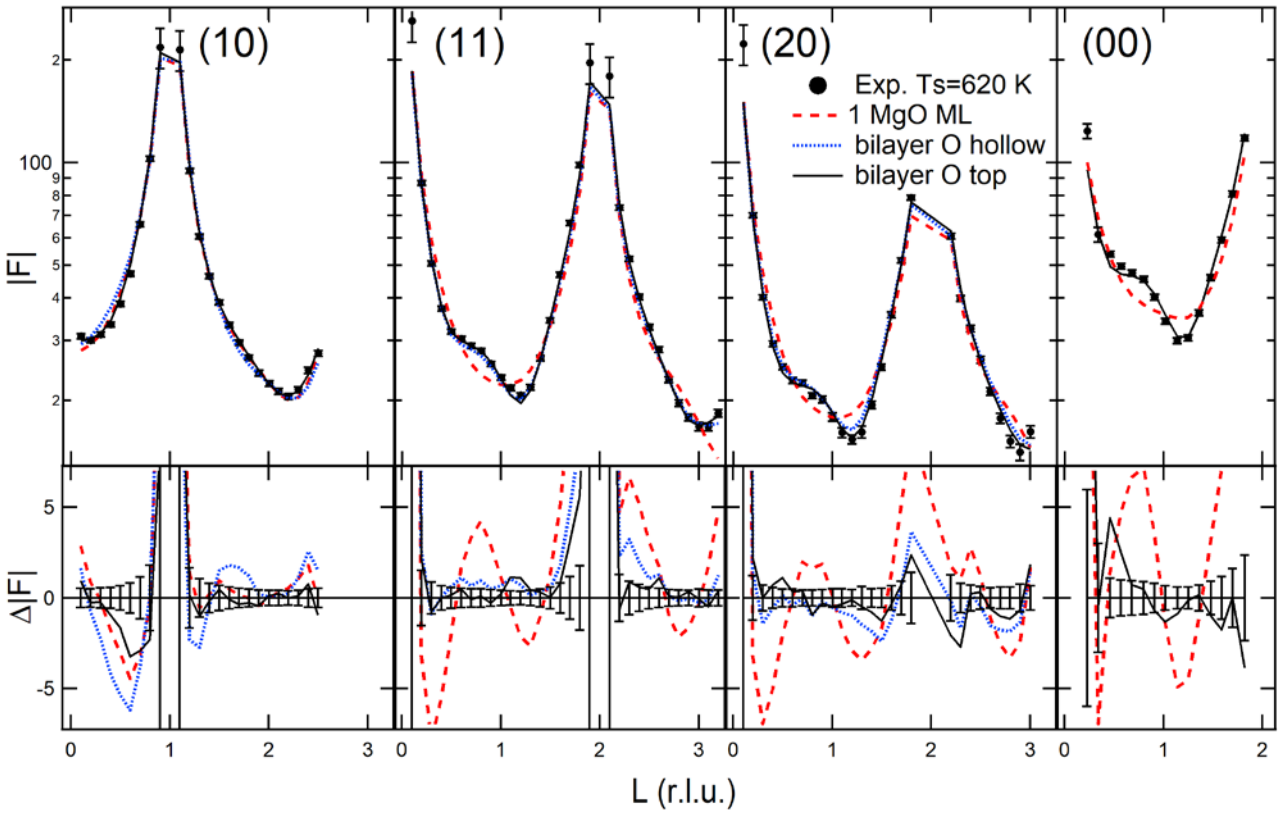

Figure 3. Upper panels: experimental MgO/Ag(001) CTRs, with error bars, for the sample grown at T_s=620 K (filled circles) and best fits for the MgO monolayer model (dashed curves, red online), the bilayer model with magnesium on top of surface Ag sites (dotted curves, blue online) and the best model with oxygen on top (black continuous lines). The error bar was increased very close to Bragg peaks to consider a systematic error, which is intrinsic in SXRD measurements collected in such a position of the rod. Lower panels: structure factor differences Δ|F| between measured and calculated structure factors for the corresponding models. They are compared with experimental error bars.

SXRD is a powerful probe of the structure of crystalline surfaces. The diffracted intensity from a truncated crystal shows, as function of the momentum transfer, a sharp scattering line-shape parallel to the surface at integer (*HK*) indexes of the surface mesh, and a continuous distribution in the out-of-plane direction in-between Bragg peaks. This out-of-plane intensity distribution is known as (*HK*) crystal truncation rod (CTR) [24]. A film, grown in registry with the substrate, gives a scattering contribution which interferes with the substrate CTR. The film structure can then be solved by a fine analysis of these CTR intensities [25].

The Ag(001) surface unit-cell is defined by the three basis vectors of a tetragonal body centred cell related to the fcc one by $\overrightarrow{a_s^1} = \frac{a_{Ag}}{2}[1\bar{1}0]$, $\overrightarrow{a_s^2} = \frac{a_{Ag}}{2}[110]$, and $\overrightarrow{a_s^3} = a_{Ag}[001]$, with a_{Ag}=408.5 pm. Data were collected using the standard method for SXRD quantitative analysis. The diffractometer axes were settled to define a (*HKL*) node of the sample's reciprocal space, and the diffracted intensity was integrated while rocking the sample around the surface normal, which results in a Δ*L* portion of the CTR crossing the detector area. The structure factor amplitudes $|F_{HKL}|$ were then extracted by applying standard correction factors [26]. Finally, the data were averaged according to the substrate's P4mm symmetry and the agreement factor between the structure factors of equivalent reflections was used as a systematic error estimation for the final experimental error calculation [27]. A set of 140 reflections, 83 of which non-equivalents, distributed along the (10), (11), and (20) CTRs, were collected for each sample, with an average agreement between the structure factors of equivalents reflections of 1.7% and 2.5% for the sample grown at 620 K and 670 K, respectively. 15 additional reflections were measured on the first sample along the specular (00) CTR, rocking in this case the incidence angle. The average MgO island size parallel to the surface was estimated by the reciprocal space width of

the (10) CTR close to the antiphase condition, measured by a rocking scan at L=0.2, corresponding to about 50 nm. The very good agreement between equivalent reflections allows for a reliable structural refinement, which is done comparing the calculated structure-factor amplitudes for trial models with the measured ones and using a χ^2 minimization to find the best model and fit parameters. The data analysis discussed in the next section was performed using the *ROD* program described in ref. [28]. Herein, all equations used in our calculations of the structure factor amplitude are reported.

3. Results and discussion

Figure 1 shows a comparison between the (10), (11), and (20) CTRs of the samples grown at 620 K and 670 K. The two datasets differ in the region in-between Bragg peaks, suggesting a different growth mode. The data of the sample grown at lower temperature show a weak bump in the middle between two Bragg peaks (full black circles). In SXRD this behavior is characteristic of a bilayer growth mode [29, 30]. The bilayer structure was confirmed by the quantitative analysis. Two trial models were tested, both consisting of a (001) MgO film with rock salt structure in epitaxy on top of the silver surface. This film is compressed in plane to match the Ag lattice constant. The first model consists of a monatomic thick MgO layer, and resulted in quite a bad agreement between simulated structure factors and data collected on the sample grown at 620 K. The χ^2 is of 22 at least in this case. The agreement improved drastically for the second model, consisting of a MgO atomic bilayer (χ^2 of 3.5). The two models are sketched in figure 2 and the best fit curves are displayed in the upper panels of figure 3. In both models the interlayer spacings $d_{Ag1\text{-}Ag2}$, $d_{Ag2\text{-}Ag3}$, and the Debye-Waller parameters B_{Ag1}, B_{Ag2}, of the two Ag atomic plane closest to the interface were optimized, together with the interface spacing $d_{MgO\text{-}Ag1}$, and a unique Debye parameter B_{MgO} for Mg and O. The last one incorporates the MgO thermal vibrations plus its structural desorder. For the bilayer, the film interlayer spacing d_{MgO} was also fitted. Finally, for both models, a roughness parameter β of the substrate [24], and the MgO covered surface fraction S_{MgO} were optimized.

The final best fit parameters are given in table 1, and will be discussed in details in the following. Let's determine the chemisorption site first. As explained, SXRD intensity is the result of the interference between the substrate and the deposited film scattering amplitudes and is therefore sensitive to their relative position. In the framework of the bilayer model, we simulated the structure factors for several chemisorption sites. The best fit discussed above, with a χ^2 of 3.5, was obtained for oxygen on top of silver and Mg on hollow sites, as shown in figure 2. This agrees with the results obtained already in early DFT calculations [31] and with photoemission experiments. In the last ones, the MgO/Ag(001) electronic structure is explained with the O 2*p* − Ag 5*sp* levels hybridization [32]. The refinement of the same film structure but with magnesium on top of Ag at the interface resulted in a relatively good qualitative agreement (dotted curve in figure 3, blue online) but in a definitively worst quantitative one with a χ^2 of 7.2. In the lower panels of figure 3 the structure factor differences $\Delta|F|$ between measured and calculated structure factors are plotted for each rod and for the three model considered. They are compared

Table 1. Best fit parameter values for the films structure obtained by deposition of about 0.8 ML of Mg on Ag(001) in 10^{-6} mbar O_2, at a substrate temperature of 620 K and 670 K. The model is sketched on the right panel of figure 2 (2 MgO ML with O on top of Ag), a third layer was added to fit the sample grown at 670 K. These values are compared to bulk and to the clean Ag(001) surface ones. $d_{Ag1\text{-}Ag2}$ and $d'_{Ag1\text{-}Ag2}$ refer to the first Ag interlayer distance in MgO covered and uncovered regions, respectively.

	T_s=620 K	T_s=670 K	Bulk	Clean Ag(001) †
$S_{MgO\text{-}1,2}$	0.38(3)	0.43(5)		
$S_{MgO\text{-}3}$	-	0.17(2)		
$d_{Ag2\text{-}Ag3}$ (pm)	205.6(4)	205.6	204.25	206(2)
$d_{Ag1\text{-}Ag2}$ (pm)	204(1)	204		
$d'_{Ag1\text{-}Ag2}$ (pm)	201(1)	201		203(2)
$d_{MgO\text{-}Ag1}$ (pm)	272(4)	271(4)	-	
d_{MgO} (pm)	214(4)	212(4)	210.65	
B_{Ag2} ($\times 10^4$ pm^2)	1.1(1)	0.9(1)	0.66	0.95
B_{Ag1} ($\times 10^4$ pm^2)	1.5(1)	1.2(1)		0.95
B_{MgO} ($\times 10^4$ pm^2)	0.9(3)	0.5(3)		
β	0.05(1)	0.07(1)		
χ^2	2.6	1.7		

† Meyerheim H L, Pflanz S, Schuster R and Robinson I K 1997 Z. Kristallogr. **212** 327

with the experimental error bars. Other interface geometries can be completely ruled out by the data analysis. This is the case for the configuration with both oxygen and magnesium atoms on bridge sites. This geometry was considered by DFT calculations, resulting in an intermediate energy in-between the former two [31]. In our SXRD analysis it gives a χ^2 of 24. We note here that the specular CTR instead is only sensitive to the interface distance and not to the chemisorption site.

The best fit bilayer model considered above results in an interface distance of about 280 pm, quite large compared to the calculated DFT values published in literature. However, up to now we fitted a unique top Ag layer position for MgO covered and uncovered regions. Indeed, we need to take into account the presence of two kind of domains, whose diffracted intensity sums up to give the measured CTRs. The first kind consists of MgO islands covered regions, the second one of uncovered Ag surface. We optimized then the first Ag interlayer spacing independently for these two regions, obtaining a better agreement with a χ^2 of 2.6. In MgO-free surface regions the spacing $d'_{Ag1\text{-}Ag2}$ is contracted by more than 1% with respect to the bulk value. This result qualitatively agrees with previous experiments on clean Ag(001) surface [33] (see table 1). Instead, in MgO covered regions this distance is bulk-like. This has an impact on the best fit interface distance $d_{MgO\text{-}Ag1}$, which is now equal to 272(4) pm. Such a value is in excellent agreement with the Ag-O distance of 270(15) pm obtained recently by EXAFS measurements [34], and with that one calculated by the same authors for a two-layer-thick MgO/Ag(001) film (271 pm). But it is somewhat larger than the values of 239(6) pm [35] and 251 pm [6] calculated previously by other groups. Indeed, it has been recently shown that calculated values spreads as function of the used functional, ranging from 249 pm to 270 pm [22]. DFT calculations indicate also a rumpling of a few pm of the interface with Mg ions closer to the surface Ag layer than O ones. Our SXRD data are not sensitive to this rumpling, which does not improve the agreement. The MgO covered surface fraction, $S_{MgO\text{-}1,2}$, is of 0.38(3), in good agreement with the calibrated deposited amount of 0.8 Mg ML. Fitting independently the coverages of the first and second MgO layer, $S_{MgO\text{-}1}$ and $S_{MgO\text{-}2}$, the same occupancy was found within an error bar of 3%. This shows that the film grown at 620 K has an almost ideal bilayer structure. The best fit substrate roughness β=0.05(1) corresponds to a R.M.S. value of about 50 pm [24]. This moderate roughness of the Ag substrate arises during the first stages of MgO epitaxial growth. The removal of Ag atoms from the substrate with the formation of monatomic islands, the formation of embedded MgO islands and carpet-like growth of the films were observed by STM [17, 18, 20]. Strain simulations performed on this system [34] revealed the existence of a small-size regime. Calculation showed that unsupported ultrathin Mg films are naturally compressed in-plane, which reduces the misfit with the Ag substrate. The out-of-plane Mg-Mg nearest neighbour distance is also slightly compressed in calculations. EXAFS measurements from the same authors confirmed this trend. For a film thickness equivalent to that one of our samples, they found an in-plane Mg-Mg interatomic distance identical to the Ag-Ag one. They also found an out-of-plane Mg-Mg nearest

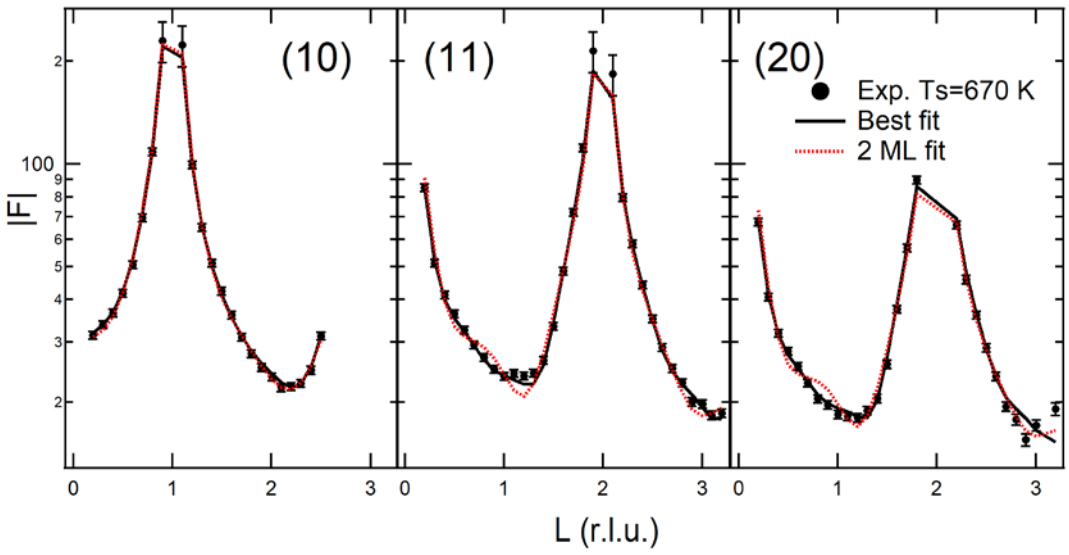

Figure 4. Experimental MgO/Ag(001) CTRs for the sample grown at T_s=670 K (filled circles), fit with the same 2 ML model of the sample grown at 620 K (dotted red lines) and best fit with a model including a 3rd incomplete MgO layer (black continuous lines).

neighbour distance of about 294 pm. This corresponds to a spacing between Mg layers of about 211 or 212 pm, slightly expanded compared to bulk. These results qualitatively agree with ours. We find a 2% expansion of the interlayer film spacing d_{MgO} with respect to the bulk, which compensates only in part the in-plane compressive strain.

Finally, we have to emphasize that the same model fits at the same time the reflectivity and the non-specular CTRs. The former is only sensitive to the electronic density perpendicular to the surface, while the latter are sensitive to films with the same in-plane lattice constant as the substrate. We can therefore exclude the presence of any significative amount of relaxed islands.

The discrepancy between the interface distance obtained here and most of the DFT calculations is in favor of the presence of extra oxygen at the interface. Accumulation of oxygen at the interface was recently demostrated, under well defined growing conditions, by a carefull comparison of STM data and DFT calculations [36]. Oxygen atoms would be located in the hollow site of the Ag top layer. The site occupancy was estimated at 10-20% for experimental conditions close to ours [37]. Calculations performed for 1 ML MgO/Ag(001), with and without the presence of 0.25 ML interface interstitial oxygen, resulted in an interface distance of about 270 pm and 250 pm, respectively [38]. This drove us to fit our SXRD data with a trial model including oxygen in this interface site. We obtain an occupancy of 0.20(6), and a position shifted outward of the Ag atomic plane by about 40 pm (to compare with about 50 pm calculated in ref. [38]), while the other parameters do not change within the error bar. However, the contribution of this interstitial oxygen to the structure factor is very weak. The χ^2 decreases only by 0.1 (to 2.5), and therefore we can neither confirm nor exclude its presence.

CTRs measured on the film grown at 670 K suggest a different morphology (figure 1). However, the quantitative analysis shows quite a bad agreement of data with a monolayer thick MgO film model (χ^2 larger than 10) meaning that the morphology is more complex. The agreement improves using the same bilayer model as for the film grown at 620 K (χ^2 ~ 5). This agreement is still unsatisfactory and the simulation shows a bump along the CTRs in the middle between Bragg peaks, which is not observed in the data (see figure 4). To fit them, a model consisting of three MgO layers needs to be considered. In this case an excellent agreement is obtained (χ^2=1.7, see figure 4). To reduce the fitting parameters, the Ag interlayer spacings of both MgO covered and uncovered regions were kept fixed to the value found for the sample grown at 620 K. Only the interface and a unique MgO-MgO interlayer spacing were optimized, giving identical results than for the 620 K grown sample, within the error bar. The only difference at 670 K is that, on top of a MgO bilayer, a third incomplete MgO layer is present, which covers almost 20% of the sample surface. ($S_{MgO\text{-}3}$=0.17(2)). This shows how sensitive the film structure is to the precise growing conditions.

4. Summary and conclusions

We have performed a SXRD investigation of the morphology and interface structure of MgO(001)/Ag(001) films about 1 ML thick. The morphology has already been investigated by several groups mainly using STM. Results are function of the specific growing conditions. Islands are formed whose size depends on the substrate temperature during elaboration [21]. Their thickness is often difficult to establish, due also to the presence of embedded MgO. Combining AFM and STM, it was shown that deposition of ~2 ML MgO/Ag(001) at T_s = 480 K results in films with coexisting 1 ML, 2 ML and 3 ML thick regions [18]. STM measurements as function of temperature support a bilayer growth mode at 1 ML coverage [21]. Another group found a transition between a multilayer structure for films grown at T_s = 500 K and monolayer islands for samples elaborated at 450 K [36]. The same authors observed nearly perfect MgO monolayers by slow cooling films grown at T_s=773 K. Cooling speed is then an essential parameter in the film growth [19]. This also supports the interpretation that multilayer growth is the thermodynamically stable phase above 500 K, which is preserved at room temperature by cooling the sample quickly enough. Here we demonstrate that reactive deposition of 0.8 Mg ML at T_s=620 K, followed by a relatively fast cooling, results in an almost perfect bilayer growth mode, with islands of ~50 nm average size. The ability of tailoring the film thickness is essential in several applications, tuning the tunnelling current between adlayers and the substrate.

SXRD is also an ideal tool to investigate the interface structure. In this way, we could provide a direct confirmation that oxygen atoms of the film are on top of silver, as overseen by DFT calculations and indirectly confirmed by photoemission experiments. We find an interface Ag-MgO interlayer distance of 272(4) pm, which is relatively large compared to DFT calculations. This distance supports the presence of additional oxygen at the interface, which we could not however confirm directly, and has an important impact on its electronic properties, and in particular on the work function.

Acknowledgements

Financial support through ANR EQUIPEX ANR-11-EQPX-0010 and beam time at the French CRG BM32 beamline of the ESRF are acknowledged. KS, VL and XT acknowledge the EU Fund for Regional Development (FEDER) through the Interreg-POCTEFA program of the Project EFA194/16/TNSI.

References

[1] Chambers S A 2000 Surface Science Reports **39** 105
[2] Repp J. Meyer G, Stojkovi S M, Gourdon A and Joachim C 2005 Phys. Rev. Lett. **94** 026803
[3] Schintke S, Messerli S, Pivetta M, Patthey F, Libioulle L, Stengel M, De Vita A, and Schneider W D 2001 Phys. Rev. Lett. **87** 276801
[4] Yuasa S and Djayaprawira D D 2007 J. Phys. D: Appl. Phys. **40** R337
[5] Wollschläger J, Erdös D, Goldbach H, Höpken R and Schröder K M 2001 Thin Solid Films **400** 1
[6] Luches P, D'Addato S, Valeri S, Groppo E, Prestipino C, Lamberti C and Boscherini F 2004 Phys. Rev. B **69**, 045412
[7] Pacchioni G and Freund H 2013 Chem. Rev. **113** 4035
[8] Yulikov M, Sterrer M, Heyde M, Rust H P, Risse T, Freund H J, Pacchioni G and Scagnelli A 2006 Phys. Rev. Lett. **96** 146804
[9] Del Vitto A, Pacchioni G, Delbecq F and Sautet P 2005 J. Phys. Chem. B **109** 8040
[10] Sterrer M, Risse T, Martinez Pozzoni U, Giordano L, Heyde M, Rust H-P, Pacchioni G and Freund H-J 2007 Phys. Rev. Lett. **98** 096107
[11] Pacchioni G, Giordano L and Baistrocchi M 2005 Phys. Rev. Lett. **94** 226104
[12] Shin H-J, Jung J, Motobayashi K, Yanagisawa S, Morikawa Y, Kim Y and Kawai M 2010 nature Materials **9** 442
[13]Hurdax P, Hollerer M, Puschnig P, Lüftner D, Egger L, Ramsey M G and Sterrer M 2020 Adv. Mater. Interfaces **7** 2000592
[14] Donati F, Rusponi S, Stepanow S, Wäckerlin C, Singha A, Persichetti L, Baltic R, Diller K, Patthey F, Fernandes E, Dreiser J, Šljivančanin Ž, Kummer K, Nistor C, Gambardella P, Brune H 2016 Science **352**, 318
[15]Wäckerlin C, Donati F, Singha A, Baltic R, Rusponi S, Diller K, Patthey F, Pivetta M, Lan Y, Klyatskaya S, Ruben M, Brune H and Dreiser J 2016 Adv. Mater. **28** 5195
[16] Peterka D, Tegenkamp C, Schröder K-M, Ernst W, Pfnür H 1999 Surface Science **431** 146
[17] Valeri S, Altieri S, del Pennino U, di Bona A, Luches P and Rota A 2002 Phys. Rev. B **65** 245410
[18] Baumann S, Rau I G, Loth S, Lutz C P and Heinrich A J 2014 ACS Nano **8** 1739
[19] Pal J, Smerieri M, Celasco E, Savio L,Vattuone L, and Rocca M 2014 Phys. Rev. Lett. **112** 126102
[20] Mechehoud F and Barth C 2015 J. Phys. Chem. C **119** 23990
[21] Ouvrard A, Niebauer J, Ghalgaoui A, Barth C, Henry C R and Bourguignon B 2011 J. Phys. Chem. C **115** 8034
[22] Prada S, Giordano L, Pacchioni G and Goniakowski J 2016 Applied Surface Science **390** 578
[23] Cabailh G, Lazzari R, Cruguel H, Jupille J, Savio L, Smerieri M, Orzelli A, Vattuone L and Rocca M 2011 J. Phys. Chem. A **115** 7161
[24] Robinson I K 1986 Phys. Rev. B **33** 3830
[25] Robinson I K and Tweet D J 1992 Rep. Prog. Phys. **55** 599
[26] Vlieg E 1997 J. Appl. Crystallogr. **30** 532
[27] Robinson I K 1991 Handbook of Synchrotron Radiation, edited by Brown G S & Moncton D E Vol. 3, p. 221. Amsterdam: North-Holland
[28] Vlieg E 2000 J. Appl. Crystallogr. **33** 401
[29]Weschke E, Schüßler-Langeheine C, Meier R, Kaindl G, Sutter C, Abernathy D and Grübel G 1997 Phys. Rev. Lett. **79** 3954
[30]Ball M J, Lucas C A, Markovic N M, Stamenkovic V and Ross P N 2002 Surface Science **518** 201
[31]Sgroi M, Pisani C and Busso M 2001 Thin Solid Films **400** 64
[32]Altieri S, Tjeng L H, and Sawatzky G A 2000 Phys. Rev. B **61** 16 948
[33] Meyerheim H L, Pflanz S, Schuster R and Robinson I K 1997 Z. Kristallogr. **212** 327
[34] Cabailh G, Goniakowski J, Noguera C, Jupille J, Lazzari R, Li J, Lagarde P and Trcera N 2019 Phys. Rev. Materials **3** 046001
[35] Giovanardi C, di Bona A, Moia T S, Valeri S, Pisani C, Sgroi M and Busso M 2002 Surf. Sci. **505** L209
[36]Savio L, Smerieri M, Vattuone L, Tosoni S, Pacchioni G, and Rocca M 2020 J. Phys. Chem. C **124** 8834
[37] Pal J, Smerieri M, Celasco E, Savio L, Vattuone L, Ferrando R, Tosoni S, Giordano L, Pacchioni G and Rocca M 2014 J. Phys. Chem. C **118** 26091
[38] Lopez N and Valeri S 2004 Phys. Rev. B **70** 125428